Planet. Space Sci., Vol. 36, No. 12, pp. 1317–1328, 1988
Printed in Great Britain.

0032-0633/88 $3.00 + 0.00
Pergamon Press plc

CONVECTION AND FIELD-ALIGNED CURRENTS, RELATED TO POLAR CAP ARCS, DURING STRONGLY NORTHWARD IMF (11 JANUARY 1983)

P. L. ISRAELEVICH, I. M. PODGORNY, A. K. KUZMIN, N. S. NIKOLAEVA and E. M. DUBININ
Space Research Institute, Academy of Sciences U.S.S.R., 117810, Moscow, Profsoyuznaya 84/32, U.S.S.R.

(*Received in final form* 20 *June* 1988)

Abstract—Electric and magnetic fields and auroral emissions have been measured by the *Intercosmos-Bulgaria*-1300 satellite on 10–11 January 1983. The measured distributions of the plasma drift velocity show that viscous convection is diminished in the evening sector under IMF $B_y < 0$ and in the morning sector if IMF $B_y > 0$. A number of sun-aligned polar cap arcs were observed at the beginning of the period of strongly northward IMF and after a few hours a θ-aurora appeared. The intensity of ionized oxygen emission [$O^+(^2P)$, 7320 Å] increased significantly reaching up to several kilo-Rayleighs in the polar cap arc. A complicated pattern of convection and field-aligned currents existed in the nightside polar cap which differed from the four-cell model of convection and NBZ field-aligned current system. This pattern was observed during 12 h and could be interpreted as six large scale field-aligned current sheets and three convective vortices inside the polar cap. Sun-aligned polar cap arcs may be located in regions both of sunward and anti-sunward convection. Structures of smaller spatial scale correspond to the boundaries of hot plasma regions related to polar cap arcs. Obviously these structures are due to S-shaped distributions of electric potential. Parallel electric fields in these S-structures provide electron acceleration up to 1 keV at the boundaries of polar cap arcs. The pairs of field-aligned currents correspond to those S-structures: a downward current at the external side of the boundary and an upward current at the internal side of it.

INTRODUCTION

Recently more attention was attracted to the polar cap phenomena during the periods of strongly northward IMF. The ionospheric current distribution obtained from groundbased magnetic data (Maezawa, 1976; Kuznetsov and Troshichev, 1977) was shown to correspond to the sunward convection in the polar cap. In the laboratory experiment (Podgorny *et al.*, 1980), an electric field appeared in the polar cap under the northward component of IMF resulting in sunward convection. This electric field was due to the merging of the magnetic field lines at the poleward sides of cusps. Measurements by the *S*3-2 satellite (Burke *et al.*, 1979) confirmed the existence of a sunward convection electric field in the center of the polar cap under IMF $B_z > 0$ and Burke *et al.* conclude that the distributions of the electric field observed at the dayside of the polar cap conform to the four-cell model of convection. Discovered by *MAGSAT* (Iijima *et al.*, 1984) the field-aligned current system NBZ also corresponds to this type of convection. It should be noted that regular distributions of the electric field and field-aligned currents corresponding to the four-cell convection were usually observed at the dayside of the summer polar cap, this fact probably being due to the influence of ionospheric conductance.

The transpolar arcs aligned along the Sun–Earth line appear in the polar cap under the northward component of IMF (Lassen and Danielsen, 1978). Their distribution and the behaviour of this distribution upon the IMF B_y sign resemble the pattern of plasma convection for IMF $B_z > 0$. The most prominent auroral phenomenon in the polar cap during northward IMF is the θ-aurora discovered by the *DE*-1 satellite (Frank *et al.*, 1982).

The θ-aurora usually assumed to correspond to convection cells and the upward field-aligned current sheet which appear in the polar cap under IMF $B_z > 0$ and/or the bifurcation of the magnetotail plasma sheet shown by computer simulation (Reiff and Burch, 1985; Kan and Burke, 1985; Ogino and Walker, 1984). However, as we know, the relationship between the θ-aurora and the polar cap convection have not yet been experimentally detected. Particularly, it should be noted that the θ-auroras were observed in the nightside of the winter polar cap where plasma convection seemed to be irregular. The comprehensive review of data related to θ-auroras has been published recently by Frank *et al.* (1986). θ-auroras correspond to the regions filled by hot plasma similar to the plasmasheet boundary layer. θ-auroras are observed in the areas both of sunward and antisunward convection. There are sufficient reasons to assume that the θ-auroras are located at the closed field lines and exist simultaneously in both hemispheres. Sim-

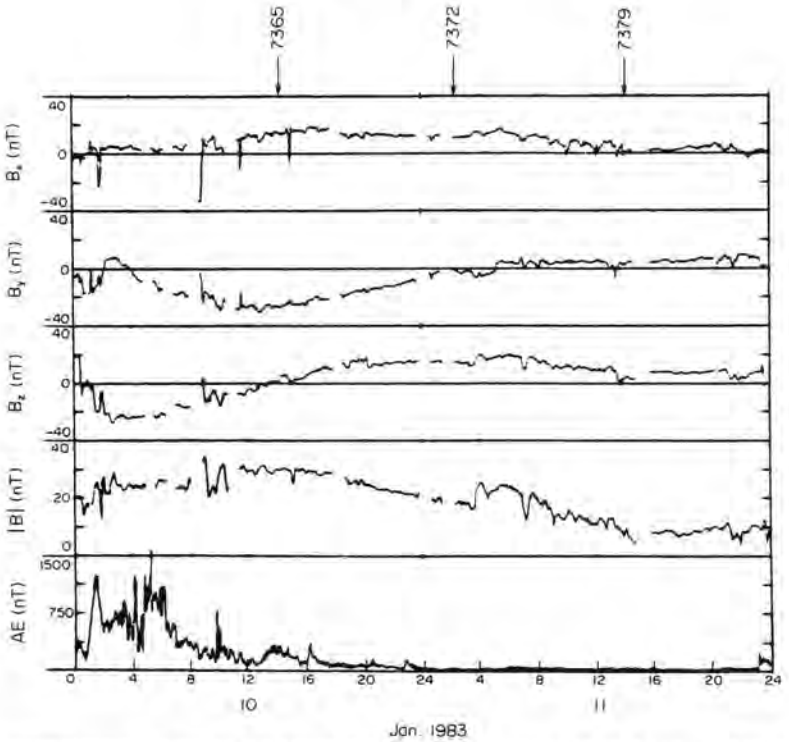

FIG. 1. THE COMPONENTS AND THE VALUE OF THE IMF AND *AE* INDEX FOR 10–11 JANUARY 1983 (AKASOFU AND TSURUTANI, 1984).
The arrows denote the measurements by the *Intercosmos-Bulgaria*-1300 satellite.

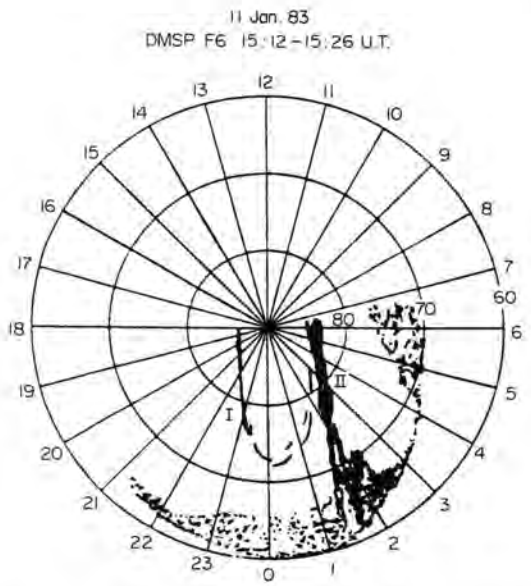

FIG. 2. THE AURORAL LUMINOSITY DISTRIBUTION IN INVLAT-M.L.T. COORDINATES AS OBSERVED BY *DMSP F*-6 AT 15:12–15:26 U.T. ON 11 JANUARY 1983 (GORNEY *et al.*, 1986).

ultaneous measurements of electron precipitation in the North and South polar caps were made by *NOAA*-7 and *DMSP F*-6 for the sun-aligned arc (Mizera *et al.*, 1987). The similarity between electron spectra and structures of penetration in both caps presume the conjugancy of the phenomena and hence the closed character of the field lines connected to the θ-aurora.

The period 10–11 January 1983 is appropriate for the studies of the phenomena related to the strong northward IMF. Unusual auroral activity was observed at this time by *DMSP F*-6 (Akasofu and Tsurutani, 1984). The magnetic field data by *ISEE*-3 are given in the same paper (see Fig. 1). Though the satellite was most probably located inside the magnetosheath near the flank of the magnetosphere, Akasofu and Tsurutani (1984) argue that these data may be used to define the direction of IMF. The auroral oval began to contract after 13:59 U.T. on 10 January (i.e. when IMF B_z became positive). At first the auroral activity was transferred to the morning sector where the oval became significantly wider than in the evening sector and surge-like structures were observed near the midnight meridian (15:37 U.T. on 10 January). Later, the auroral oval luminosity

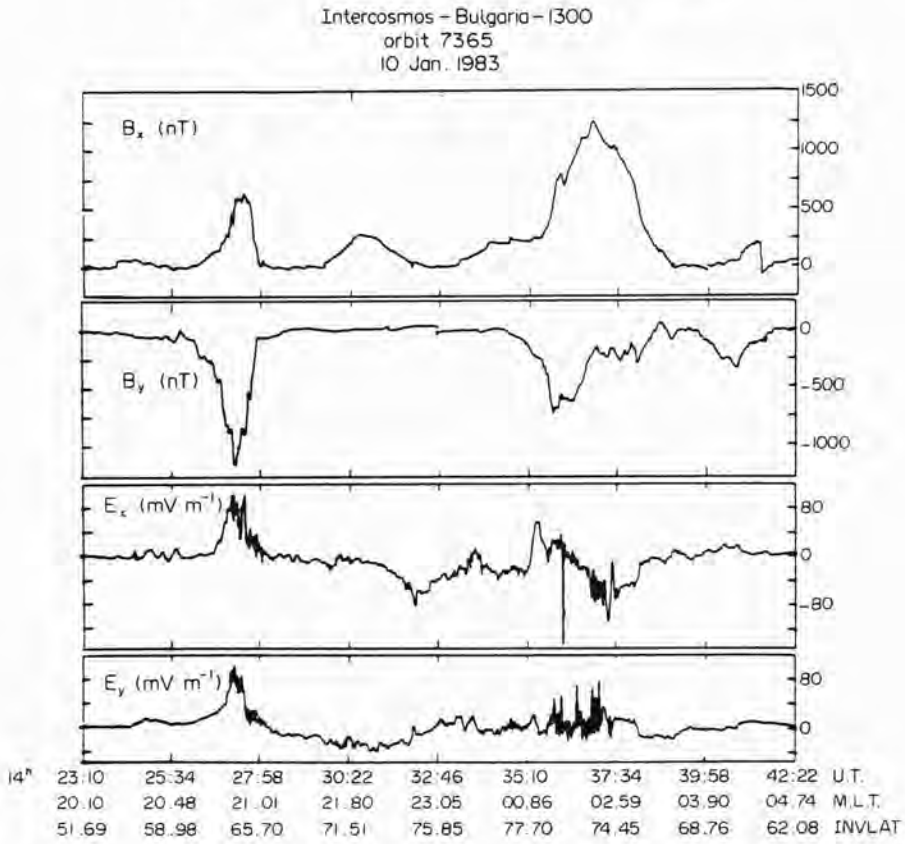

FIG. 3. THE COMPONENTS OF THE MAGNETIC FIELD DISTURBANCE ΔB_x, ΔB_y AND OF THE ELECTRIC FIELD E_z AND E_y AVERAGED PER 0.96 S FOR THE ORBIT 7365 (14:23–14:42 U.T. ON 10 JANUARY 1983).

decreased and sun-aligned arcs appeared in the polar cap while B_z grew and B_y diminished. At least 15 arcs were observed at 06:53 U.T. on 11 January. Later, a wide arc (resembling θ-aurora) was seen in the polar cap at 15:00 U.T. on 11 January (Fig. 2). Measurements of electron and ion fluxes made by *DMSP F-6*, *NOAA-6* and *NOAA-7* satellites during this period showed that the plasma inside the transpolar arc was similar to the plasma in the morning sector of the auroral oval (Gorney *et al.*, 1986) and, as the authors presumed, originated from the same source. A significant enhancement of precipitating ions and electron fluxes accompanied the transpolar arc. The acceleration of the electrons was observed at both boundaries of the arc. Measurements of precipitating particles indicated simultaneous existence of the polar cap arc in the Southern Hemisphere.

The hot plasma was observed over the sun-aligned polar arcs and it is reasonable that its precipitation explains auroral luminosity. However, the electron spectra at the boundaries of the hot plasma region (Gorney *et al.*, 1986; Mizera *et al.*, 1987) show the electron acceleration up to 1 keV.

Three sequences of measurements by the *Intercosmos-Bulgaria*-1300 satellite are available for the period 10–11 January 1983. They are denoted by arrows in Fig. 1. These measurements present a possibility to evaluate the distribution of magnetic and electric fields together with the intensities of auroral emissions along the orbit during the turning of the interplanetary magnetic field to the North. Unfortunately, the measurements of electron and proton spectra have not been made during these sequences. In this paper we analyze the data on the magnetic and electric fields and auroral emissions to relate the polar cap arcs to the specific features of the electric and magnetic fields.

The *Intercosmos-Bulgaria*-1300 satellite was launched on 7 August 1981 into a nearly circular orbit at an altitude of 900 km and an inclination of

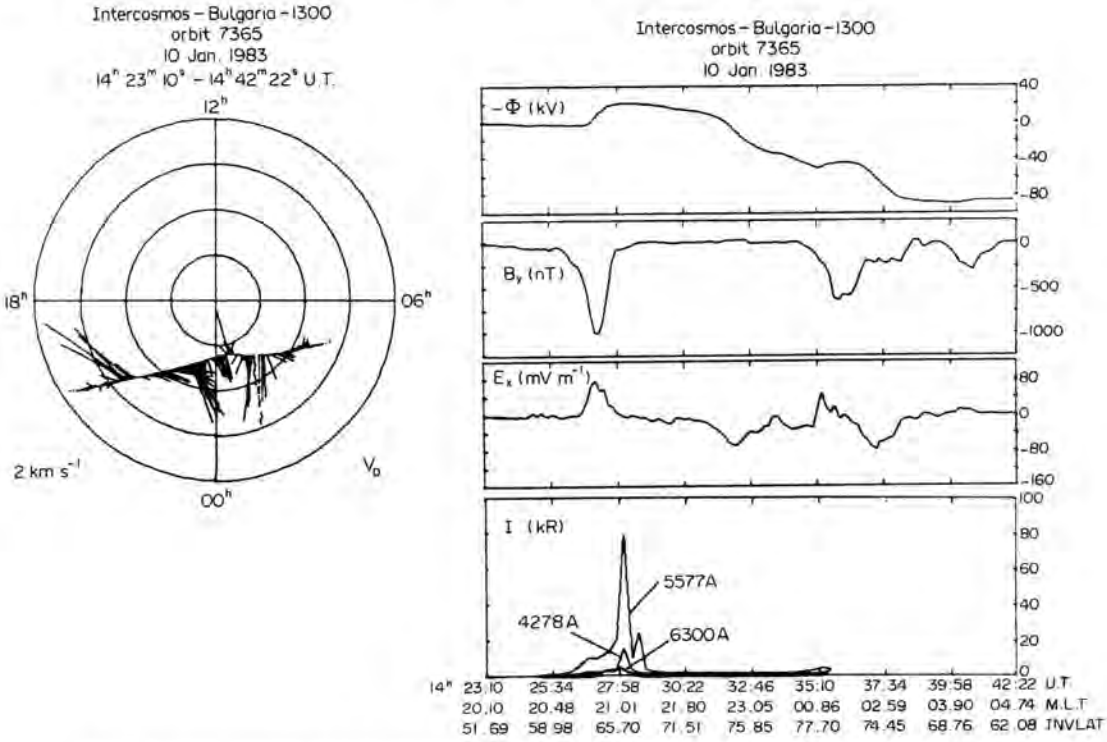

FIG. 4. AT LEFT: DISTRIBUTION OF THE DRIFT VELOCITY VECTORS ALONG THE ORBIT 7365 IN INVLAT-M.L.T. COORDINATES.
At right: electric potential Φ, magnetic field disturbance ΔB_y, electric field component E_x averaged per 4.8 s and auroral luminosity intensity for the orbit 7365.

81°. The spacecraft was three-axis stabilized with an orientation accuracy to 1°. The scientific instrumentation was described by Serafimov *et al.* (1981). Here we shall try to interpret the data on electric and magnetic fields and auroral luminosity in different spectral lines. The measurements of the fields were made with a sampling rate of 0.08 s and the intensity of luminosity was measured every 16 s for each spectral line. The right-hand orbital coordinate system was defined as follows: X-axis was aligned along the velocity vector and Z-axis was along the radius-vector of the spacecraft from the Earth.

EXPERIMENTAL RESULTS

Distributions of transversal components of electric field **E** and magnetic field disturbance **ΔB** averaged per 0.96 s along the orbit 7365 are presented in Fig. 3. The measurements were made at 14:23–14:42 U.T. on 10 January, when the IMF B_z was close to zero and the IMF B_y component dominated. The component of magnetic field disturbance ΔB_y reveals a pair of intense field-aligned currents in the evening sector (the downward current at the equatorward portion and the upward current at the poleward portion of the oval). These currents correspond to the common regions 1 and 2 of the evening sector. At the morning side the pattern of field-aligned currents becomes more complicated as compared with the common two-sheet structure. Here four large-scale field-aligned current sheets can be seen: the downward current (14:34:34–14:35:46 U.T.), the upward current (14:35:46–14:38:45 U.T.), the downward current (14:38:45–14:40:46 U.T.) and the upward current (14:40:46–14:41:34 U.T.). Obviously, the auroral activity in the morning oval observed by *DMSP F*-6 is related to the wide upward current sheet at 14:35:46–14:38:45 U.T.

The electric field distribution shows common sunward convection inside the regions 1 and 2 of field-aligned currents and antisunward convection further to the pole in the evening sector. An enhancement of antisunward convection (significant decrease of E_x component at 14:31:34–14:33:22 U.T.) is observed in

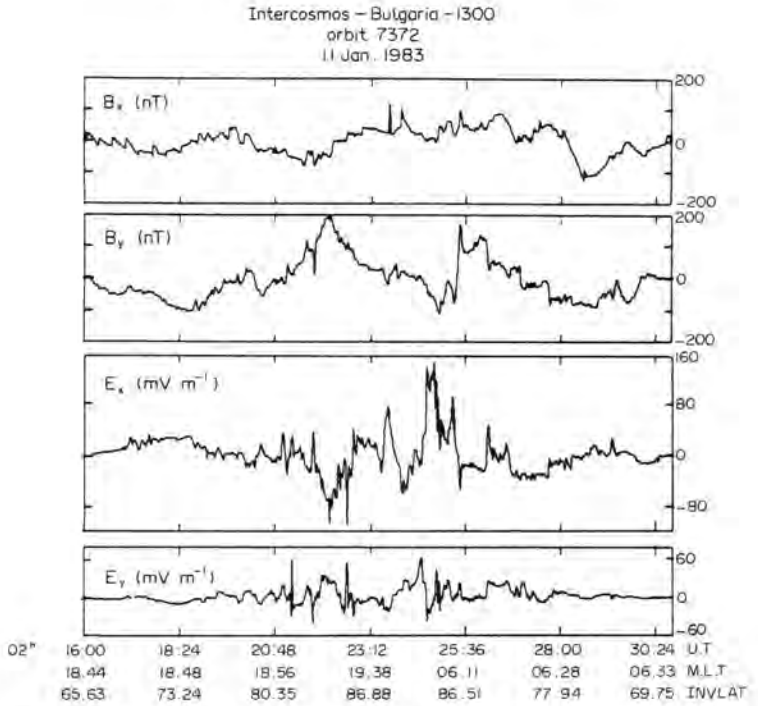

FIG. 5. THE SAME AS IN FIG. 3 FOR THE ORBIT 7372 (02:16–02:30 U.T. ON 11 JANUARY 1983).

the polar cap. However, these changes in E_x are not accompanied by variations of ΔB_y (i.e. by field-aligned currents). The convection pattern is more complicated at the morning side. A narrow band of sunward convection is observed at the poleward boundary of the oval (14:36:10–14:35:40 U.T.), an intensive antisunward convection is observed further at lower latitudes and only insignificant sunward fluxes can be seen in the equatorial portion of the oval. The pattern of plasma convection is presented in Fig. 4, where the distribution of drift velocity vectors along the orbit is shown at the left and distributions of potential, Φ, components of electric (E_x) and magnetic (ΔB_y) fields averaged per 4.8 s and intensities of the upper atmosphere emissions in 5577, 4278 and 6300 Å are given at the right. The photometer was switched off in the morning sector after the spacecraft left the shadow. The luminosity distribution in the evening oval has a common character: diffusive emissions in the region of the downward current and intensive discrete luminosity in the upward current sheet. (When comparing the photometer data to the measurements of fields one should take into account that the photometer line of sight was directed vertically downward and there is a time delay between the registration of the field-aligned currents and corresponding auroral emission due to the inclination of the magnetic field line to the local vertical. This time delay was 15–20 s for this orbit in the evening sector.) This fact draws attention to one that there is a significant potential difference of the order of 60 kV along the given part of the orbit, i.e. the antisunward flow is not compensated by sunward flows. This is also clearly seen from the distribution of the drift velocity vectors in Fig. 4.

The next seance was made in the orbit 7372 at 02:16–02:30 U.T. on 11 January, when the IMF B_y was small and negative and IMF $B_z > 0$. A number of sun-aligned arcs was observed by *DMSP F*-6 at this time.

Figure 5 presents the data on electric field components E_x, E_y and magnetic field disturbance components ΔB_x, ΔB_y. The magnitude of magnetic field disturbances (i.e. the intensity of field-aligned currents) is significantly smaller than in the previous seance. The remnants of region 1 and 2 of field-aligned currents are observed in the evening (00:217:12–02:19:36 U.T.) and in the morning (00:227:50–02:30:20 U.T.) sectors. The value of the ΔB_y reaches

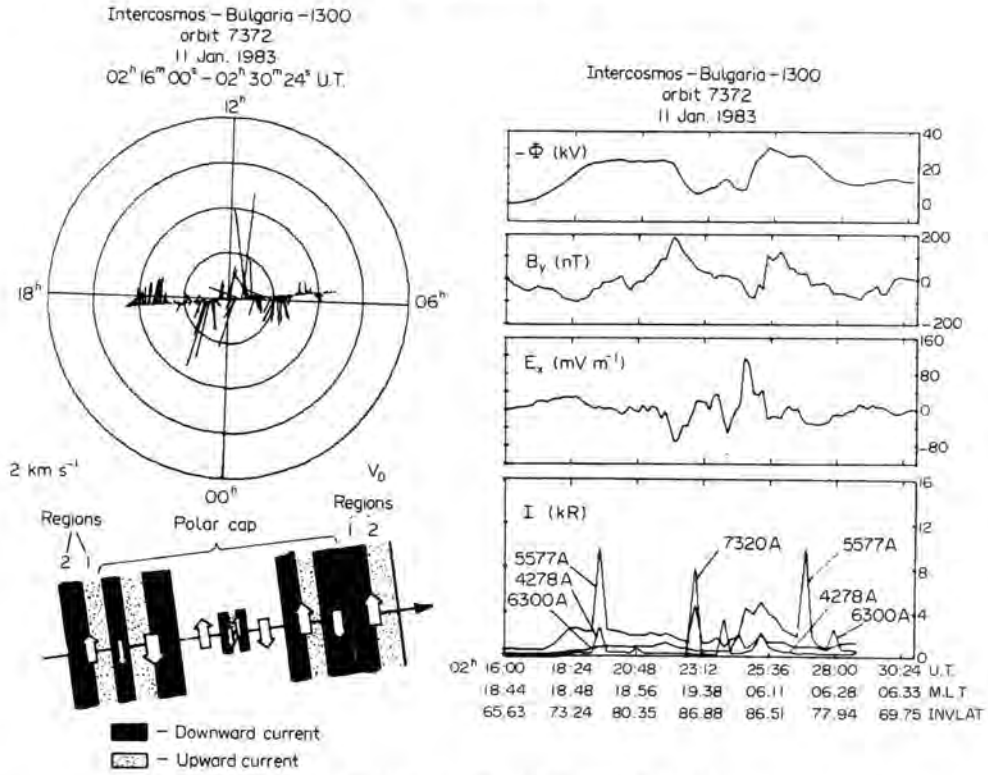

FIG. 6. THE SAME AS IN FIG. 4 FOR THE ORBIT 7372.
At left: at bottom a pattern of current sheets and convection directions is shown schematically for this orbit.

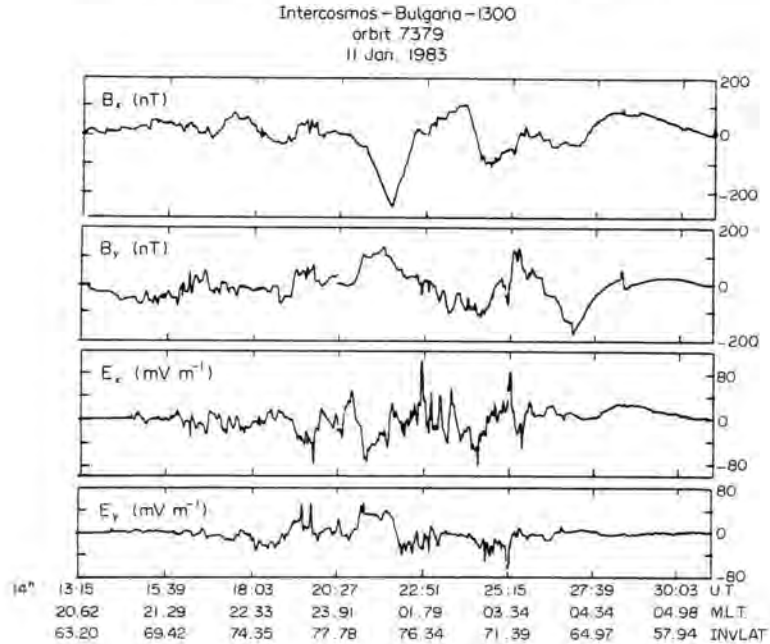

FIG. 7. THE SAME AS IN FIG. 3 FOR THE ORBIT 7379 (14:13–14:30 U.T. ON 11 JANUARY 1983).

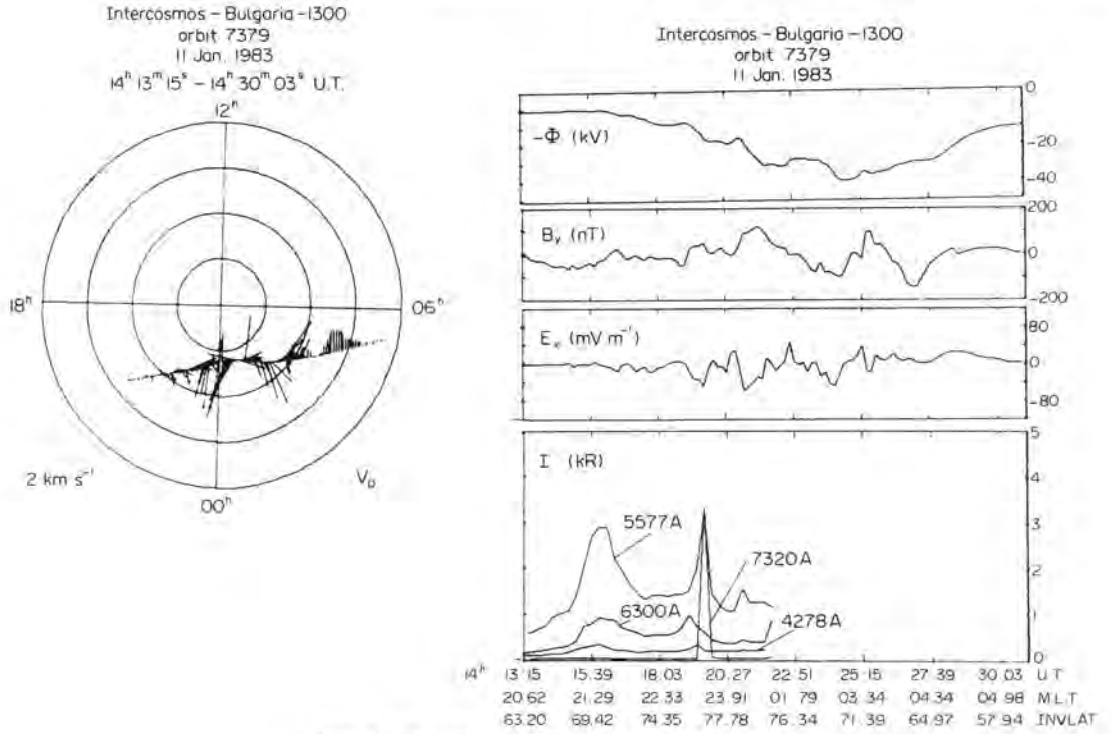

FIG. 8. THE SAME AS IN FIG. 4 FOR THE ORBIT 7379.

only 100 nT, so field-aligned currents in the auroral zone are an order of magnitude smaller than in the orbit 7365. Field-aligned currents appear in the polar cap (ΔB_y reaches 200 nT), but their distribution is more complicated and differs from the W-shaped distribution typical for NBZ field-aligned current system (Iijima *et al.*, 1984). This is quite natural because the measurements were made in the winter polar cap at the nightside. There are two large scale structures of polar cap field-aligned currents each consisting of three current sheets. These are in the evening side: the downward current (02:20:10–02:20:32 U.T.), the upward current (02:20:32–02:22:10 U.T.), the downward current (02:22:10–02:23:00 U.T.) and in the morning side: the downward current (02:24:32–02:24:58 U.T.), the upward current (02:24:58–02:25:55 U.T.), the downward current (02:22:55–02:27:12 U.T.). These current sheets are sun-aligned as the main magnetic field disturbance is in ΔB_y and the orbit is along the dusk-down meridian.

Figure 5 shows that during the northward IMF intense electric fields (higher than 100 mV m^{-1}) appear in the polar cap. Strong sunward convection is observed (positive values of E_x correspond to sunward drift). The antisunward convection dominates in the region of three large scale field-aligned current sheets in the evening sector and in the morning side polar cap field-aligned currents region the convection is mainly sunward. The strong convection both sunward and antisunward near the pole (02:23:50 U.T.) is accompanied by small field-aligned currents. The sunward convection is observed in the area of remnants of field-aligned current regions 1 and 2. This pattern of convection is given in Fig. 6, where drift velocity vectors V_D, potential Φ, field components E_x and ΔB_y and emissions intensities in 6300, 5577, 4278 and 7320 Å are shown in the same format as in Fig. 4. At the bottom of Fig. 6 the relation between the field-aligned currents and convection direction is presented schematically.

Data on auroral luminosity reveal typical regions of diffusive and discrete emissions in the evening oval similar to those observed in the previous seance, but weaker by an order of magnitude. A number of arcs (no less than eight) are observed inside the polar cap. The most interesting feature of these data is the sharp increase of emission of ionized oxygen OII (^{2}P) 7320 Å up to 9 kR in one of the arcs (02:23:00 U.T.).

During the last sequence the measurements were made at 14:13–14:30 U.T. on 11 January in the orbit 7379. B_z component of IMF was strong and northward and B_y component was positive. Figure 2 shows

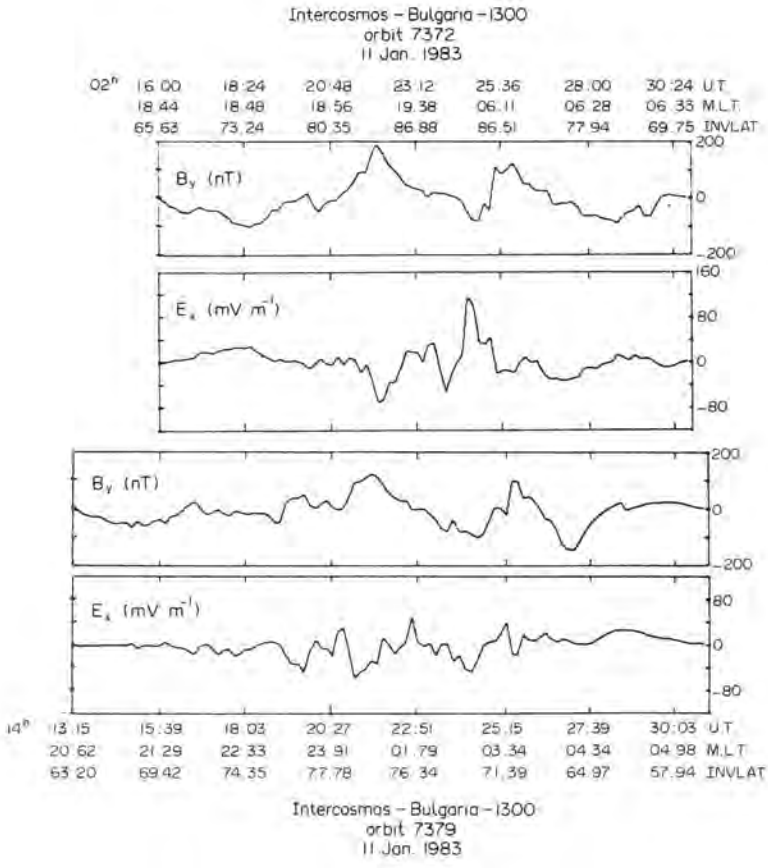

FIG. 9. AVERAGED PER 4.8 s COMPONENT ΔB_y OF MAGNETIC FIELD DISTURBANCE AND ELECTRIC FIELD COMPONENT E_x FOR THE ORBIT 7372 (AT THE TOP) AND FOR THE ORBIT 7379 (AT THE BOTTOM).

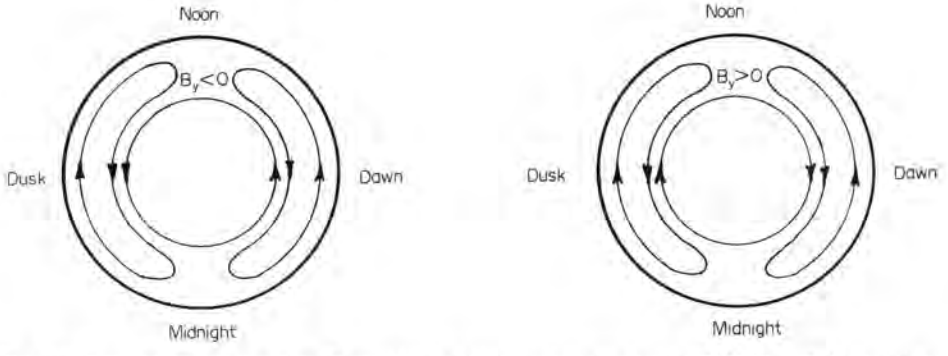

FIG. 10. SCHEMES OF VISCOUS AND B_y-DEPENDENT CONVECTIVE CELLS UNDER IMF $B_y < 0$ (AT LEFT) AND IMF $B_y > 0$ (AT RIGHT).

the luminosity pattern typical for θ-aurora obtained by *DMSP F*-6 one hour later.

Figure 7 presents the distributions of E_x, E_y, ΔB_x and ΔB_y electric and magnetic field components. A rather complicated pattern of field-aligned currents in the polar cap is observed here as in the previous seance. There are significant disturbances of the ΔB_x component for the orbit 7379, so here current sheet

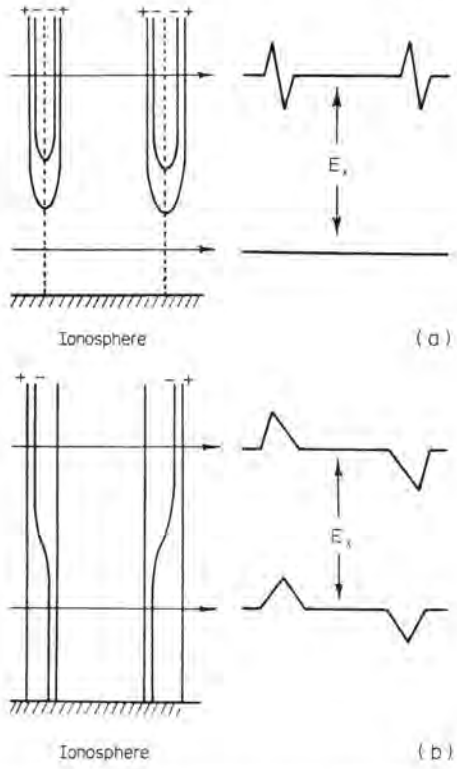

FIG. 11. SCHEMES OF ELECTRIC POTENTIAL DISTRIBUTIONS AT THE BOUNDARIES OF THE PLASMA STRUCTURE RELATED TO THE SUN-ALIGNED POLAR ARC.
At left: a pattern of equipotentials; at right: distributions of the electric field along the orbits crossing the plasma structure above the acceleration region and below it. (a) The case of V-shaped potential distribution. (b) The case of S-shaped potential distribution.

directions deflect from Sun–Earth line.

The electric field distribution reveals several narrow bands of sunward convection in the polar cap. The electric field magnitude (i.e. convection velocity) is lower than for the orbit 7372. This may be due to the changes of external conditions or to the fact that the orbit 7379 was located farther to the nightside than the orbit 7372. Drift velocity vectors along the orbit 7379 are shown in Fig. 8 alongside with the distributions of potential, field components E_x and ΔB_y and luminosity intensities. A comparison between distributions of potential for the orbits 7372 and 7379 show their different behaviour. Opposite signs of Φ for these two orbits mean that drift velocity vectors along the orbits cannot be simply combined into a single convection pattern.

The intensity of diffuse and discrete luminosity in the evening sector diminishes three times with respect to that of the orbit 7372. Only one arc is observed in the polar cap obviously corresponding to the arc I in Fig. 2. The photometer was switched off before the satellite entered the region of the arc II. Here also a significant enhancement of OII emission in line 7320 Å is observed within the arc I.

DISCUSSION

No evident relationship between the sun-aligned polar arcs and large scale field-aligned currents and convection can be envisaged from the data presented above. However, before we try to search for structures of smaller scale related to the arcs we shall make a few brief remarks about the observed electric and magnetic field distributions.

Rather complicated distributions of the electric field and field-aligned currents were observed for the orbits 7372 and 7379. Nevertheless, a certain similarity can be observed between the distributions of ΔB_y along these orbits (Fig. 9). One should note that the distribution for the orbit 7379 is somewhat shifted to the morning side. The similarity between the distributions of E_x is not so evident, but it can also be seen especially in the evening side. Obviously we deal with a rather stable system of several (probably three) vortices.

Another feature is the distribution of electric potential along these orbits. Both these distributions are symmetric with respect to the day–night line, but potentials have opposite signs for these two orbits. Such symmetric distributions of potential presume the existence of large-scale circulation of the drift velocity vector. It seems strange, at first sight, that the circulation direction is opposite to that observed in the polar cap for different signs of IMF B_y component. The circulation is clockwise for the orbit 7372 (IMF $B_y < 0$) and counterclockwise for the orbit 7379 (IMF $B_y > 0$). However, distributions of drift velocity vectors (see Figs 6 and 8) show that the difference in the sign of electric potential is due to the vanishing sunward convection in the morning side for the orbit 7372 and in the evening side for the orbit 7379. So the evening or morning viscous convection cell vanishes depending upon the direction of IMF B_y. Actually, the same was observed for the orbit 7365 where the pattern of convection was strongly modified in the morning sector for IMF $B_y < 0$. Figure 10 clarifies why the interaction between the viscous cells and B_y dependent cell is most intensive in the morning side for $B_y < 0$ and in the evening side for $B_y > 0$. The interaction intensifies when the drift velocities become opposite in different cells.

Let us try to find a structure of the electric field responsible for the sun-aligned polar arc. Frank *et al.*

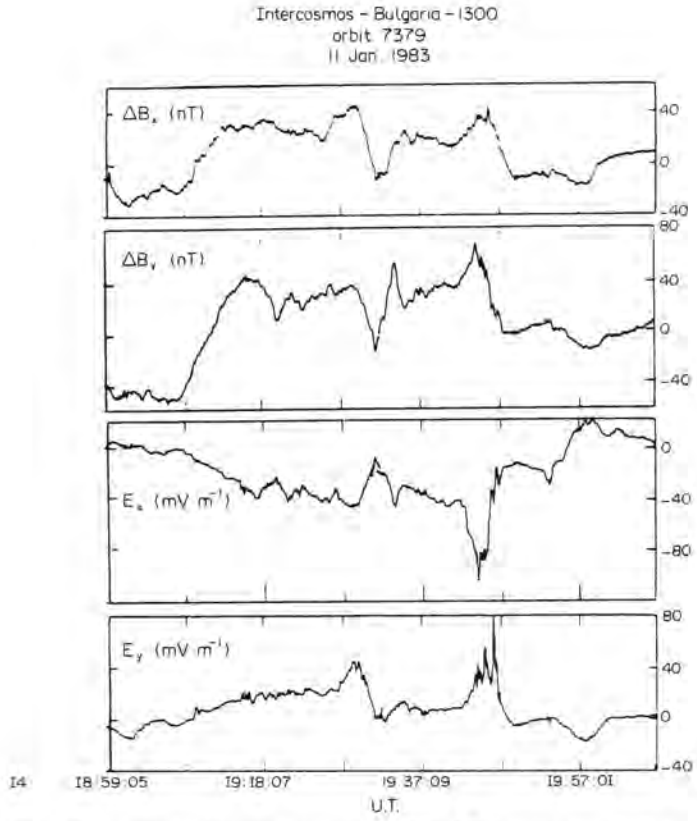

FIG. 12. COMPONENTS OF THE MAGNETIC FIELD DISTURBANCE ΔB_x, ΔB_y AND ELECTRIC FIELD COMPONENTS E_x, E_y MEASURED WITH SAMPLING RATE 0.08 S INSIDE THE REGION OF ARC I (SEE FIG. 2) IN THE ORBIT 7379 (14:18:59–14:19:57 U.T. ON 11 JANUARY 1983).

(1986) and Gorney *et al.* (1986) show that polar cap arcs are related to the regions of the hot plasma ($T_e \sim 200$ eV, $T_i \sim 2$ keV) similar to the plasma of the plasmasheet boundary layer. It is possible that recently discovered plasma formations in the tail lobes (Huang *et al.*, 1987; Dubinin *et al.*, 1988) also correspond to the polar cap arcs. We note that the similarity between plasma parameters in these regions and in the plasmasheet boundary layer does not necessarily prove their origin from PSBL while such an origin seems to be most probable. However, it is possible in principle that these plasma regions have another source and their similarity to the plasma sheet boundary layer is due to some similarity in mechanisms of formation of these structures and the plasmasheet.

An electron acceleration up to 1 keV was observed at the boundaries of the plasma structures related to transpolar arcs (Gorney *et al.*, 1986), i.e. narrow regions of parallel electric fields existed along both boundaries of these plasma structures providing the potential difference of 1 kV. Of course, numerous different patterns of potential distribution may be proposed to explain the appearance of the parallel electric field. We shall consider two rather simple cases of V- and S-shaped distributions of the electric potential at the boundary of the hot plasma region. Figure 11 shows equipotentials for both cases. At the right, the distributions of the electric field are shown along the orbits crossing the plasma structure above and below the acceleration region.

Figure 12 presents the measurements of the electric and magnetic fields with a sampling rate of 0.08 s made within the region of arc I (see Fig. 2) (14:18:59–14:19:57 U.T., orbit 7379). It is impossible to make a detailed comparison of electric and magnetic data with the position of the arc, firstly, because of the relatively low sampling rate of optical measurements and, secondly, due to the inclination of the magnetic field lines to the local vertical. However, a structure of the electric field is clearly established in Fig. 12 which could be predicted for the S-shaped electric potential distribution at the boundaries of the hot plasma region (Fig. 11b). The maximum of the electric

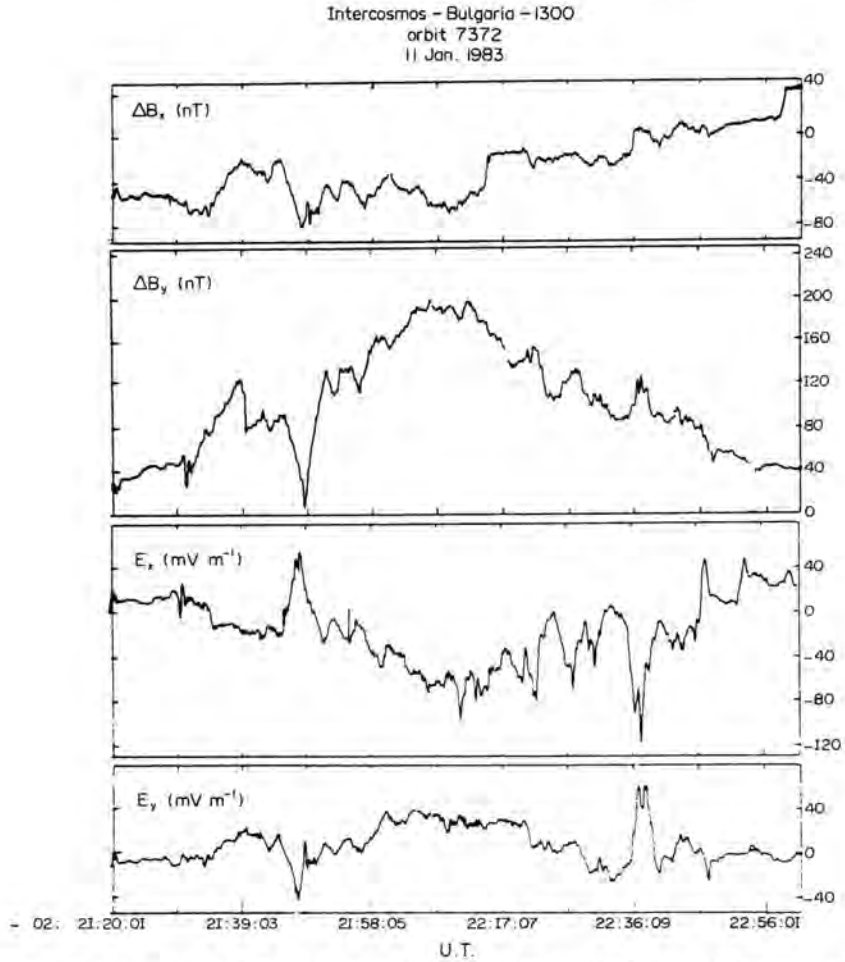

FIG. 13. THE SAME AS IN FIG. 12 FOR THE ORBIT 7372 (02:21:20–02:22:56 U.T. ON 11 JANUARY 1983).

field at 14:19:32 U.T. corresponds to the entrance into the plasma structure and the minimum at 14:19:44 U.T. corresponds to the exit from the structure. Corresponding potential differences at the boundaries are 0.8 kV (at entrance) and 1.2 kV (at exit) and agree well with the observations of accelerated electrons (Gorney *et al.*, 1986). The magnetic field disturbance correlates with the electric field, meaning that pairs of field-aligned currents exist at the boundaries of the plasma structure. The current is downward at the external side of the boundary and upward at its internal side. The agreement of the observed structure with the pattern of two S-shaped potential distributions is partially disturbed by the presence of the minimum of E_x and small downward current at 14:19:34 U.T. However, this discrepancy may be caused by transient processes. As a whole this structure is observed at the background of the electric field of a larger scale $E_x \sim -40$ mV m^{-1}, so this structure drifts from the Sun. Such structures may probably drift to the Sun also. Some ideas on the evolution of this structure and its stability can be envisaged by comparing the data on electric and magnetic fields with the same sampling rate measured near the region of enhanced luminosity in line 7320 Å (obviously developed later into arc I) in the orbit 7372. The behaviour of the electric field typical for S-shaped distributions of potential can be clearly seen in Fig. 13. The distance between two S-shaped distributions (02:21:47 and 02:22:36 U.T.), that is transversal scale of the structure, is larger for this case. It is 360 km for the orbit 7372 and 90 km for the orbit 7379. The following mechanism of appearance of the electric field normal to the boundary, which in its turn gives rise to a parallel electric field, is possible: hot ions may penetrate outside through the plasma boundary due to their large

Larmor radius. This leads to the electric field of necessary sign normal to the boundary. The magnitude of this field is defined by ion temperature as this polarization field in its turn prevents the ion penetration through the boundary. The electric potential jump at the boundary should be of the order of T_i which is also in agreement with the observations of accelerated electrons.

CONCLUSIONS

Measurements made by the *Intercosmos-Bulgaria*-1300 satellite on 10–11 January 1983 have shown the following.

(1) A complicated pattern of convection and field-aligned currents was observed in the nightside of winter polar cap during strongly northward IMF. This pattern differs from the four-cell convection model and NBZ field-aligned current system. It indicates the existence in the polar cap of six large scale field-aligned current sheets and three convective large scale vortices. The polar cap arcs may be situated both in the sunward convection regions and in the areas of antisunward convection.

(2) The structures of the electric field of smaller scale are observed at the boundaries of sun-aligned polar arcs. These structures obviously correspond to S-shaped electric potential distributions. Parallel electric fields in these S-shaped distributions provide electron acceleration up to 1 keV at the boundaries of the polar arc.

(3) The pairs of field-aligned currents accompany electric field structures at the boundaries of the sun-aligned polar arc. The current is downward at the external side of the boundary and is upward at the internal side.

(4) Significant enhancement of ionized oxygen emission (7320 Å) up to several kilo-Rayleighs was observed in the polar cap arc.

(5) The interaction between viscous and B_y-dependent convection cells leads to the vanishing of viscous convection in the morning sector under IMF $B_y < 0$ and in the evening side under $B_y > 0$.

REFERENCES

Akasofu, S.-I. and Tsurutani, B. (1984) Unusual auroral features observed on 10–11 January 1983 and their possible relationships to the interplanetary magnetic field. *Geophys. Res. Lett.* **11**, 1086.

Burke, W. J., Kelley, M. C., Sagalyn, R. C., Smiddy, M. and Lai, S. T. (1979) Polar cap electric field structure with a northward interplanetary field. *Geophys. Res. Lett.* **6**, 21.

Dubinin, E. M., Zakharov, A. V., Pissarenko, N. F., Lundin, R. and Hultquist, B. (1988) The plasma mantle study. 4—Standing plasma structures. Kosmich. issled. (in press).

Frank, L. A., Craven, J. D., Burch, J. L. and Winningham, J. D. (1982) Polar views of the Earth's aurora with *Dynamic Explorer*. *Geophys. Res. Lett.* **9**, 1001.

Frank, L. A., Craven, J. D., Gurnett, D. A., Shawhan, S. D., Weimer, D. R., Burch, J. L., Winningham, J. D., Chappell, C. R., Waite, J. H., Heelis, R. A., Maynard, N. C., Sugiura, M., Petersen, W. K. and Shelley, E. G. (1986) The Theta aurora. *J. geophys. Res.* **91**, 3177.

Gorney, D. J., Evans, D. S., Gussenhoven, M. S. and Mizera, P. F. (1986) A multiple-satellite observation of the high-latitude auroral activity on 11 January 1983. *J. geophys. Res.* **91**, 339.

Huang, C. Y., Frank, L. A., Peterson, W. K., Williams, D. J., Lennartsson, W., Mitchell, D. G., Elphic, R. C. and Russell, C. T. (1987) Filamentary structures in the magnetotail lobes. *J. geophys. Res.* **92**, 2349.

Iijima, T., Potemra, T. A., Zanetti, L. J. and Bythrow, P. F. (1984) Large-scale Birkeland currents in the dayside polar region during strongly northward IMF: a new Birkeland current system. *J. geophys. Res.* **89**, 7441.

Kan, J. R. and Burke, W. J. (1985) A theoretical model of polar cap auroral arcs. *J. geophys. Res.* **90**, 4171.

Kuznetsov, B. M. and Troshichev, O. A. (1977) On the nature of polar cap magnetic activity during undisturbed periods. *Planet. Space Sci.* **25**, 15.

Lassen, K. and Danielsen, C. (1978) Quiet time pattern of auroral arcs for different directions of the interplanetary magnetic field in the *Y–Z* plane. *J. geophys. Res.* **83**, 5277.

Maezawa, K. (1976) Magnetospheric convection induced by the positive and negative components of the interplanetary field: quantitative analysis using polar cap magnetic records. *J. geophys. Res.* **81**, 2289.

Mizera, P. F., Gorney, D. J. and Evans, D. S. (1987) On the conjugancy of the aurora: high and low latitudes. *Geophys. Res. Lett.*, **14**, 190.

Ogino, T. and Walker, K. J. (1984) The magneto-hydrodynamic simulation of the bifurcation of the tail lobes during intervals of northward IMF. *Geophys. Res. Lett.* **11**, 1018.

Podgorny, I. M., Dubinin, E. M. and Potanin, Yu. N. (1980) The magnetospheric boundary's magnetic field. *Geophys. Res. Lett.* **5**, 247.

Reiff, P. H. and Burch, J. L. (1985) IMF B_y-dependent plasma flow and Birkeland currents in the dayside magnetosphere. 2—A global model for northward and southward IMF. *J. geophys. Res.* **90**, 1595.

Serafimov, K., Kutiev, I., Gogoshev, M., Bochev, A., Dachev, Ts., Ivanov, I., Adasko, V., Balebanov, V., Iosifyan, A., Podgorny, I. and Sheremetyevsky, N. (1981) New complex for ionosphere–magnetosphere study *Intercosmoc-Bulgaria*-1300. Preprint IAF 81-212.